



Graphene-Based Nanomaterials and Their Applications in Biosensors

4

Young Jun Kim and Bongjin Jeong

4.1 Graphene

4.1.1 Key Properties of Graphene

Graphene has been drawing tremendous attraction since the crystal graphene had been first observed by Novoselov in 2004 based on scotch-tape method (Novoselov et al. 2004). The name of the one-atom thick 2-D material, graphene is composed of two concepts, graphite and -ene. The thickness of graphene is the separation distance of the graphite, which is 0.335 nm recording the thinnest among all the nanomaterials developed until now. Graphene is 100–300 times stronger than steel with its Young's modulus of 0.5–1.0 TPa and intrinsic strength of 130 GPa (Lee et al. 2008). The electron mobility at room temperature is $2.5 \times 10^5 \text{ cm}^2 \text{ V}^{-1} \text{ s}^{-1}$ (Mayorov et al. 2011) with its maximum current density reaching a few million times larger than copper (Liu et al. 2007). The single atom thick crystal material has high thermal conductivity of 3000 WmK^{-1} (Balandin et al. 2008) and high optical transmittance of 97.7% (Nair et al. 2008). Rightly these superb properties contributed Nobel Prize for Physics in 2010 and have been widely

used for applications including sensors, electronics, energies and biology.

Two approaches are usually applied for the synthesis of graphene, bottom-up and top-down methods. In bottom-up method graphite is oxidized under very harsh condition to produce well-dispersed graphene oxide in aqueous medium, which in turn reduced to graphene. However, the reduction process does not produce completely -reduced graphene form. The chemical process generates graphene with some defects causing to be called reduced graphene oxide instead of graphene. In the top-down method chemical vapors are crystalized on a proper substrate form single-layer graphene. However, this is not suitable for mass production process. Many different types of exfoliation methods have been developed due to advantages of producing large amount of graphene in a relatively simple process.

4.1.2 Mechanical Exfoliation

The first discovery of graphene was processed based on mechanical exfoliation method using graphite, in which graphene is stacked together linked by van der Waals force. Although the van der Waals force itself is weak the force between graphenes in graphite is very strong since the van der Waals force works all over the surface of graphene. In order to produce graphene through

Y. J. Kim (✉) · B. Jeong
BioMedicalIT Department, Electronics and
Telecommunications Research Institute (ETRI), Daejeon,
South Korea
e-mail: junkim@etri.re.kr; bjj0919@etri.re.kr

exfoliation the van der Waals force is the first thing to overcome. Also another point to consider in exfoliation is lubricating effect in the lateral direction.

Sonication turned out to be a useful tool in exfoliation process due to advantage of producing large amount of graphene. When sonicated graphite powder is dispersed in solvents such as N, N-dimethylformamide (DMF) or N-methylpyrrolidone (NMP). However due to limit in dispersibility of graphene in those solvents, the concentration of graphene produced from sonication exfoliation is usually too low (~ 0.01 mg/mL) to be of any practical use. When the difference in surface energy between graphene and solvent is minimum, exfoliation tends to occur more easily. From the mechanistic point of view exfoliation is facilitated by liquid cavitation which in turn generates micro-bubbles. When the bubbles explode around the graphite the impulse helps to generate exfoliation process (Ciesielski and Samori 2014). However, sonication process has been reported to generate oxygen containing defects such as aldehyde, carboxylic acid, and ethers (Skaltsas et al. 2013).

Ball milling is another way for exfoliating graphite into graphene. In contrast to the sonication method where normal force is the major contributor, in the ball milling process shear force is the dominant factor. Another factor of force in the ball milling process is the balls which act on graphite through collisions. The ball milling can be processed either by wet or dry condition. In the wet process typically graphite is dispersed using solvents that are in good match with the surface energy of the graphite. Although mostly DMF and NMP are used as the matching solvents, combined use of 1-pyrenen carboxylic acid and methanol turned out to result in more efficient exfoliation than DMF alone (Aparna et al. 2013).

In spite of the scalability in production, the above-mentioned mechanical methods for exfoliation have to be developed to produce enhanced yield in monolayer graphene. Fragmentation effects also have to be reduced. In the case of sonication many interacting factors such as power, frequency, and time have to be optimized.

Also defects of the graphene has to be minimized and uniformness of the product has to be enhanced.

4.1.3 Synthesis of Graphene

Although many different processes for exfoliation have been developed for large-scale production, the peeling-off method cannot avoid defects especially when it comes to producing large-scale graphene. Synthetic methods have been reported to be advantageous in this respect (Dreyer et al. 2010; Choi et al. 2010). Chemical vapor deposition (CVD) has been mostly widely used due to processibility of generating single-layer graphene over relatively large area (Li et al. 2009). For example, centimeter-scale graphene was able to be produced on a copper substrate using CVD method. Chemical synthetic method for graphene has also been widely used since the chemical wet process is suitable for large production. In the chemical process graphite is oxidized to produce graphene oxide (GO), which in turn is chemically reduced to reduced form of graphene oxide (rGO) (Li et al. 2008). Since the quality of rGO in the chemical synthetic method depends largely on the efficiency of reduction process, many different methods and reducing agents have been developed to obtain high quality rGO.

4.1.4 Characterization of Graphene

As described in the exfoliation and synthetic method for graphene, the product is usually a mixture of a single- and multi-layer of graphene. Many of the characterization methods for graphene is focused on the differentiating those species. Since, in the chemical synthetic method, GO is reduced to rGO, differentiation between these species and degree of reduction are critical aspects to be understood.

UV-visible spectroscopy can be used to identify GO and rGO. GO is characteristic of two absorption maxima (λ_{MAX}) at 234 nm and 299 nm. The shorter λ_{MAX} is attributed to $\pi-\pi^*$ transition in the aromatic C=C bonds while the

longer λ_{MAX} is caused by $n-\pi^*$ transition in C=O bonds. In the case of rGO, λ_{MAX} appears at 269 nm which corresponds to $\pi-\pi^*$ transition in the aromatic C=C bonds. The red shift of $\pi-\pi^*$ transition in the aromatic C=C bonds for rGO indicates more delocalization of p-orbitals when GO is reduced to rGO (Paredes et al. 2008)

Raman spectroscopy is an efficient tool to identify pristine graphite, GO and rGO. Pristine graphite shows a very sharp G peak at 1581 cm^{-1} , which is caused by the in-plane vibration in the sp^2 carbons. When graphite is oxidized, the G peak shifts to 1589 cm^{-1} in somewhat broadened mode and disordered structural pattern of GO, which has been caused by oxidation, produces a D band at 1352 cm^{-1} (Wang et al. 2009a, b, c). When GO is reduced to rGO, the G peak blue-shifts to 1582 cm^{-1} which is close to the G peak from the pristine graphite. Therefore the relative peak intensity between D and G can be used to understand the degree of defect in graphene.

XPS can be effectively used to understand the extent of reduction of GO. Since oxidized form of carbons in GO occurs as C-O (ethers and hydroxyls) and C=O (carbonyl) in addition to C-C (unoxidized carbons), C atoms in GO reveals at three different energies, 284.6 eV for C-C, 286.7 eV for C-O and 288.4 eV for C=O.

Atomic force microscopy (AFM) is a useful tool to identify single-layer graphene, of which thickness is reported to be $0.32 \sim 1.2\text{ nm}$. More accurate way to characterize single-layer graphene than AFM is transmission electron microscopy (TEM), in which observation of transparency and edge of the graphene directly reveals whether the graphene is single-layered, double-layered or triple-layered, as well statistical analysis of the thickness (Hernandez et al. 2008).

4.1.5 Functionalization of Graphene

Even though graphene has great potential for applications in electronics, sensors, and various composites, in order to be of any practical utility, some barriers have to be overcome such as zero band gap, low dispersibility and inertness to chemical modifications. Many different methods

for functionalizing graphene have been developed to enhance the real applicability of graphene. Functionalization on graphene can be processed either through covalent bonding or through non-covalent bonding. In this review functionalization of graphene will be focused mainly on method via covalent bonding. From the organic chemistry point of view, the chemical reactions can generally be processed by condensation reaction, addition reaction and substitution reaction, which can also be subdivided into nucleophilic and electrophilic substitution reactions.

In the condensation-type modification of graphene, thionyl chloride (SOCl_2) chemistry is widely used to enable further functionalization on graphene. GO, which contains diverse oxygen-containing functional groups such as hydroxyl, epoxy and carboxylic groups is a good starting point to initiate functionalization process. The carboxylic acid on GO was reacted with SOCl_2 to generate $-\text{COCl}$ group which is labile to various types of nucleophiles. Indeed, alkylamine (RNH_2) was reacted with $-\text{COCl}$ to produce amide bond ($-\text{CONHR}$). Now the functional group R is linked with GO through amide bond, enabling the product with easy dispersibility in various types of solvents including THF, carbon tetrachloride (CCl_4) and dichloroethane (Niyogi et al. 2006). Isocyanate compound (RNCO) has been used to prepare amide bond ($-\text{CONHR}$) via reaction with carboxylic acid. Also the functionalization enables compatibility of GO with various polymers to produce graphene-polymer composite (Stankovich et al. 2006).

Different from condensation reaction which is mostly carried out via GO, addition reaction on graphene turned out to be a useful tool to enable direction chemical modification on graphene. Diazonium salt is an effective compound to carry out functionalization on graphene via free radicals which can be generated by heating the diazonium compound. Based on this chemistry, nitrophenyl diazonium compound ($\text{BF}_4^- \text{N}_2^+ \text{C}_6\text{H}_4\text{-NO}_2$) was reacted on graphene to produce nitrophenyl group. The addition reaction turned out to affect conductivity of graphene by transforming sp^2 carbons to sp^3 carbons. Based on this, conductivity of graphene was able to

adjusted in a controlled manner, which in turn generated band gap on graphene making possible of applications as semiconducting materials (Sinitiskii et al. 2010; Niyogi et al. 2010).

Substitution reactions can occur at epoxy groups on GO using diverse types of nucleophilic functionalities. Primary amine groups are good candidate for the purpose. Amines with varying length of alkyl groups ($C_nH_{2n}NH_2$) were used to add alkyl groups on GO (Bourlinos et al. 2003). When the alkyl chain was relatively short ($n = 2, 4, 8, 12$) the reaction was able to proceed at room temperature. However, when the alkyl chain was long ($n = 18$) the reaction had to be refluxed to complete the reaction.

4.2 Graphene Quantum Dots (GQDs)

Graphene quantum dot (GQD) is a graphene fragmented within around 20 nm. Although semiconductor quantum dots (SQDs) have been attracting much attention, more diverse and wider applications of GQDs are limited due to problems related with cost, toxicity, biocompatibility and chemical modification. In contrast, GQDs are understood to be superior to SQDs with those problems. In this section synthetic methods and optical properties of GQDs are described.

4.2.1 Synthesis of GQDs

GQDs are generally prepared in two approaches, top-down and bottom-up. In the top-down method GQDs are prepared by exfoliating graphite followed by fragmentation step. The top-down method involves harsh reaction conditions and produces GQDs with irregular morphology and wide size distribution. Graphite is usually a starting material and is converted into GO using a modified version of the Hummers procedure (Hummers and Offeman 1958), in which sulfuric acid, sodium nitrate and potassium permanganate are involved. In the case of bottom-up method

very uniform GQDs are produced. However, bottom-up preparation of GQDs involves complex synthetic steps.

Many different top-down methods have been developed and the major difference among them is how GO is converted into GQDs. Hydrothermal cutting is one of the widely used top-down methods, in which relatively strong basic compounds such as NaOH are used as scissors for the carbon precursors. Pan et al. prepared GQD with diameter of 5–13 nm in aqueous media by thermally reducing GO to graphene and chemical oxidation of the graphene followed by hydrothermal reduction to GQD (Pan et al. 2010). From a mechanistic point of view, oxidation process generates epoxy groups in linear fashion along carbon lattice, which upon further oxidation are converted to carbonyl groups. Under hydrothermal conditions the linear mode of oxidation acts as a defect site for to be cut to produce GQDs.

Solvothermal method was used to produce GQDs. GO in DMF was sonicated and heated at 200 °C to produce GQDs with average diameter of 5.3 nm and thickness of 1.2 nm indicating most of the GQDs are in single layered or bi-layered state. The resulting GQDs displayed strong fluorescence with photoluminescence quantum yield of 11.4% (Zhu et al. 2011).

Microwave has been utilized for synthesizing GQDs (Li et al. 2012; Zhu et al. 2010; Chen et al. 2010, 2012). Use of microwave has advantage over the hydrothermal and oxidation procedure by providing high energy rapidly and uniformly throughout the reaction medium which results in short reaction time and enhanced uniformity of GQDs. One-pot microwave approach in the absence of stabilizer was reported to produce greenish yellow luminescent GQDs from GO (Li et al. 2012). Epoxy groups were oxidized to form a line of mixture of functional groups composed of minor amount of epoxy and majority of carbonyl groups. The greenish yellow luminescent GQDs were mostly single and bi-layered graphene with average diameter of 4.5 nm with photoluminescence (PL) quantum yield of 11.7%. By treating the GQDs with

NaBH₄ blue-luminescent GQDs were obtained almost without change in dimension with PL quantum yield of 22.9%.

Electrochemical methods also have been used to prepare GQDs (Li et al. 2011; Zhang et al. 2012) based on anode oxidation and anion intercalation which in turn help exfoliate carbon anode. When graphite is used as a working electrode in the preparation of carbon dots, the high redox potential ranging from ± 1.5 V to ± 3 V can oxidize carbon-carbon single bond enabling oxidative cleavage (Lu et al. 2009). Also potential cycling allows the involving electrolytes to be intercalated into carbon anode. Zhang reported high yield process by exfoliating graphite based on electrochemical method. Dependency of the functionalization mode on temperature was reported. When the hydrazine reduction was processed at ambient temperature, reduction was exerted mostly on basal epoxy and hydroxyl groups. However, when the temperature was increased the reduction produced amidation on the edge carboxylic groups leading to hydrazide formation between two adjacent carboxylic groups.

In a bottom-up method, a polycyclic aromatic molecule, hexa-peri-hexabenzocoronene, was pyrolyzed, oxidized and functionalized followed by reduction to produce GQDs (Liu et al. 2011). Yan et al. produced GQDs by oxidizing dendritic polyphenylene precursors. In order to provide solubility of the resulting GQDs phenyl rings were substituted with 3 long alkyl groups (Yan et al. 2010).

4.2.2 Luminescence Properties of GQDs

According to the calculation based on density function theory, the energy gap of GQDs of $\pi - \pi^*$ transition decrease as the size of GQDs increase (Eda et al. 2010). Depending on the way a graphene sheet is cut along the crystallographic direction, the edges can form zigzag or armchair mode. It is reported that types of edges

affect the optoelectronic and magnetic properties of GQDs. Such size-dependent properties arise from quantum confinement effect (Chan and Nie 1998; Michalet et al. 2005; Smith and Nie 2010). In general, the smaller GQDs display luminescence at shorter wave length (Freeman and Willner 2012).

Also PL of GQDs tend to be affected by pH (Pan et al. 2010; Zhu et al. 2012). While hydrothermally prepared GQDs under basic condition display strong PL, GQDs prepared under acidic conditions show negligible PL. Under acidic conditions protonation of the zigzag edges disrupts the emissive triplet carbene state. In contrast under basic condition detachment of protons from the zigzag edges revive PL. Also PL patterns are affected by solvents and concentration of GQDs (Fan et al. 2012).

4.3 Applications of Graphene for Biosensors

4.3.1 Introduction

Many different types of sensing systems have been developed in order to maximize detection performance as well as to minimize handling procedures and the size of the sensors. Since electrical and fluorescent properties are the most prominent characteristics of graphene derivatives, sensing systems based on electrochemical and fluorescent properties of graphene have been much studied.

Use of graphene as an electrode in electrochemical applications has advantage in catalytic efficiency which is superior to that of carbon nanotube (CNT) with wide range of electrochemical potential of 2.5 V in 0.1 M PBS at pH 7.0 (Alwarappan et al. 2009). Graphene has lower - charge-transfer resistance than graphite and glass carbon electrodes (GCEs) (Zhou et al. 2009). Electrical properties of were investigated for different redox systems, Ru(NH₃)₆^{3+/2+}, Fe(CN)₆^{3-/4-}, Fe^{3+/2+} and dopamine (Tang et al. 2009). Two different electrodes were compared, bare

glassy carbon (GC) and glassy carbon modified with rGO sheet film (rGSF). Much faster apparent electron-transfer rate constant (k° app) was observed on rGSF than on GC for both Ru(NH₃)₆^{3+/2+}, Fe(CN)₆^{3-/4-}.

4.3.2 Graphene-Based Immunosensors

Immunoassay takes advantage of the interaction between antibody and antigen. Enzyme-linked immunoassay (ELISA) is a standard clinical diagnostic method, in which a capture antibody is in complexation with an antigen and a detection antibody in a sandwich-type fashion. One of the key factors for high sensitivity in electrochemical detection is how efficient the electron transfer is on the electrode surface. Highly conductive property of graphene is well suited for this purpose and much application has been developed to enhance the electrical conductivity on electrode surface by using graphene as surface modification medium. Many different types of protein-based cancer biomarkers have been detected using electrochemical immunoassay. Alpha-fetoprotein (AFP), a biomarker for hepatocellular cancer, was assayed on graphene-modified electrode in the hope of enhancing sensing performance by facilitating electron transfer rate of the electrode using graphene (Du et al. 2010).

Ultrasensitive immunoassay was processed by generating polyaniline (PAN) via catalysis with Horse-radish peroxidase (HRP)-conjugated AuNP (HRP-AuNP) (Fig. 4.1) (Lai et al. 2014). In the presence of poly(diallyldimethylammonium chloride) (PDDA) GO was reduced by hydrazine to produce composite of rGO/PDDA. AuNPs were mixed with the composite of rGO/PDDA to prepare rGO/AuNP. The rGO/AuNP was dispersed in water to be dropped on the screen-printed carbon electrode (SPCE), onto which anti-human IgG(anti-HIgG) was added. Due to high surface area of the rGO/AuNP nanocomposite provides large amount of anti-

HIgG may be position, which would lead to highly sensitive assay system. In order to process immunoassay, HIgG was added followed by HRP-conjugated AuNP to form sandwich-typed complexation. Aniline monomer and H₂O₂ were added to form PAN. The aniline monomers are polymerized through catalysis by HRP oxidation of aniline by HRP-AuNP. Thus produced PAN is electrochemically determined for immunoassay. The nanocomposite system was reported to be able to detect 9.7 pg/mL of IgG with dynamic range covering 4 orders of magnitude. Such a high sensitivity is reported to have been contributed by the amplification effect of HRP-AuNP and the acceleration of electron transfer by rGO/AuNP.

Ultrasensitive electrochemical immunoassay system (limit of detection 100 fg/mL, 700aM) was reported using rGO (Fig. 4.2) (Monsur et al. 2012). Indium tin oxide (ITO) electrode was functionalized with amine group using amine-functionalized benzenediazonium. The amine functionalized ITO surface was coated with GO, in which the primary amine on the ITO surface was reacted with carboxylic acid positioned at the edge of GO. Then the GO on the ITO surface was electrochemically reduced to prepare rGO on ITO surface. Using π - π interaction of the aromatic rings positioned between ITO surface and polymer, the N-acryloxysuccinimide-functionalized poly(BMA-r-PEGMA-r-NAS) was coated on the rGO surface. IgG was tethered on the polymer coating through reaction of the primary amines in IgG with N-succinimide in the polymer. Then ELISA was processed via sandwich-type complexation with antigen and HRP-labeled secondary anti-IgG.

GQDs were used for immunoassay taking advantage of the unique luminescent and resonance energy transfer (RET) properties of GQDs to recognize 10 ng/mL of human IgG (Fig. 4.3) (Zhao et al. 2013). When mouse anti-human immunoglobulin G (mIgG) functionalized GQDs came in contact with graphene, the luminescent GQDs became quenched through π - π *

Fig. 4.1 Schematic view of the preparation for ultrasensitive detection of IgG based on rGO/AuNP system. (Lai et al. 2014. Copyright © Lai et al.)

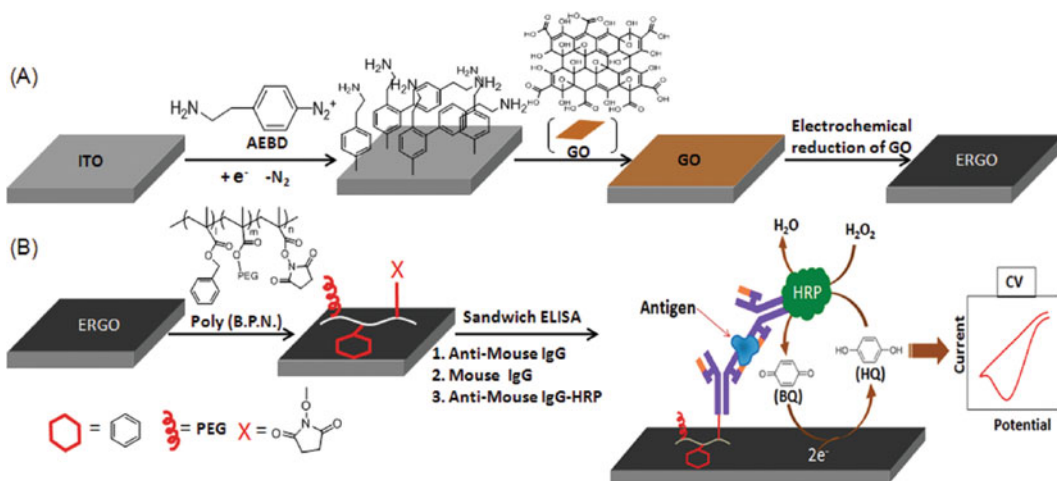
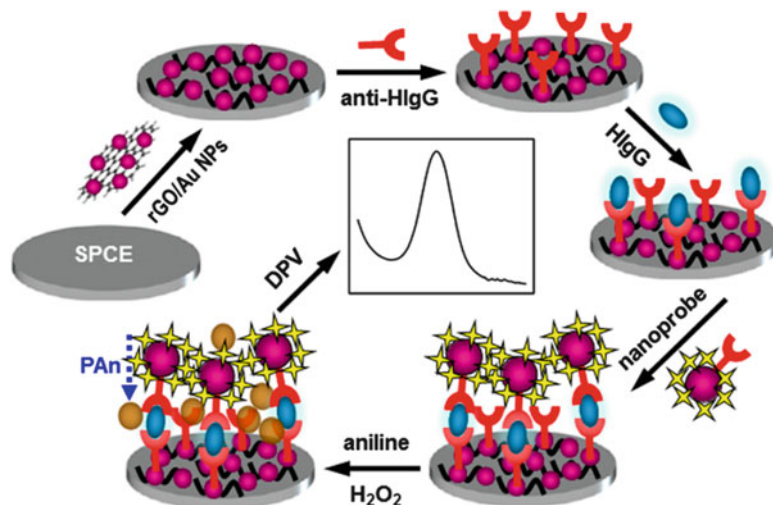


Fig. 4.2 Schematic view of the preparation and working principle for the ultrasensitive electrochemical immunoassay. (Monsur et al. 2012 Copyright © Monsur et al.)

stacking interaction. To this quenched system human IgG was added to restore some degree of luminescence caused by interruption of the π - π^* stacking interaction due to the intervening IgG.

4.3.3 Graphene-Based Detection of Oligonucleotides

DNA also can be recognized on graphene-based electrode via electrochemical analysis. Graphene-based electrode can catalytically oxidize the four

DNA bases, A, G, C, and T, enabling direct detection of a single-nucleotide polymorphism (SNPP in a short oligonucleotide (Zhou et al. 2009). Immobilization of single-strand DNA were processed either through adsorption or covalent bonding. Simple adsorption of single-strand DNA were processed on GO or rGO. Reduction of GO was processed electrochemically (Giovanni et al. 2012), thermally (Yang et al. 2013) or polyaniline-electrochemically (Wang et al. 2011). Covalent immobilization of DNA was processed by reacting amine-functionalized

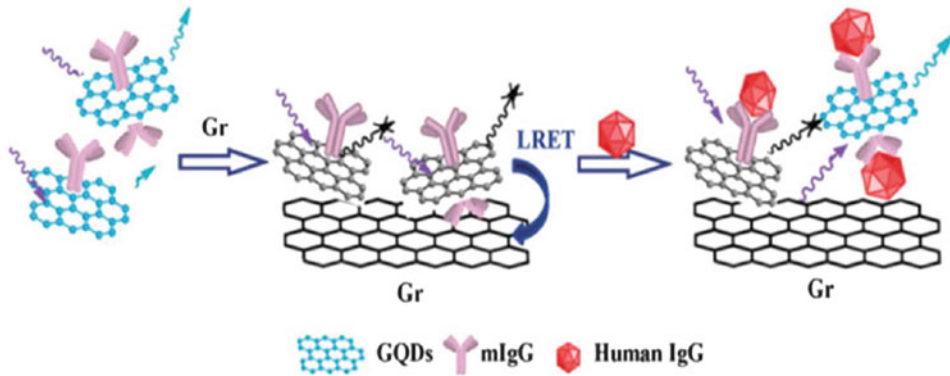


Fig. 4.3 GQD as an immunoassay system via luminescence resonance energy transfer (LRET). (Zhao et al. 2013. Copyright © Zhao et al.)

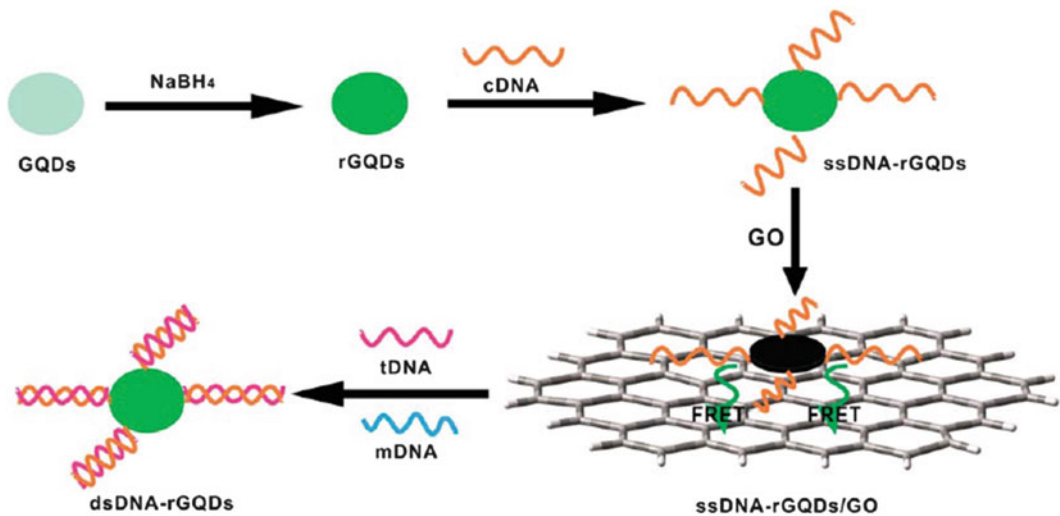


Fig. 4.4 GQDs-based DNA detection system based on fluorescence resonance energy transfer (FRET). (Qian et al. 2014. Copyright © Qian Z S et al.)

DNA on the oxygen containing rGO via carbodiimide (Bonanni et al. 2012).

Quain et al. reported fluorescence resonance energy transfer (FRET)-based DNA assay with limit of detection (LOD) of 75 pM and dynamic range of 6.7 ~ 46 nM (Fig. 4.4). (Qian et al. 2014). GQDs were treated with NaBH_4 to produce reduced GQDs (rGQDs), which can fluoresce prominently. Single-strand DNA (ssDNA) probes were tethered on rGQDs (ssDNA-rGQDs) through condensation reaction. The ssDNA-rGQDs came in contact with GO through π - π interaction leading to fluorescence quenching.

When target DNA was added to form double-strand DNA (dsDNA), the dsDNA interrupts the π - π interaction to detach ssDNA-rGQDs from GO leading to restoring of fluorescence.

Zhang et al. presented a molecular beacon (MB)-based miRNA detection system utilizing GQDs (Fig. 4.5) (Zhang et al. 2015). Molecular beacons are oligonucleotides designed with stem and loop structures (Broude 2002; Wang et al. 2009a; Stobiecka and Chalupa 2015; Tang et al. 2009). The oligonucleotides are equipped with a fluorophore at one end and a quencher at the other. MicroRNAs were able to be

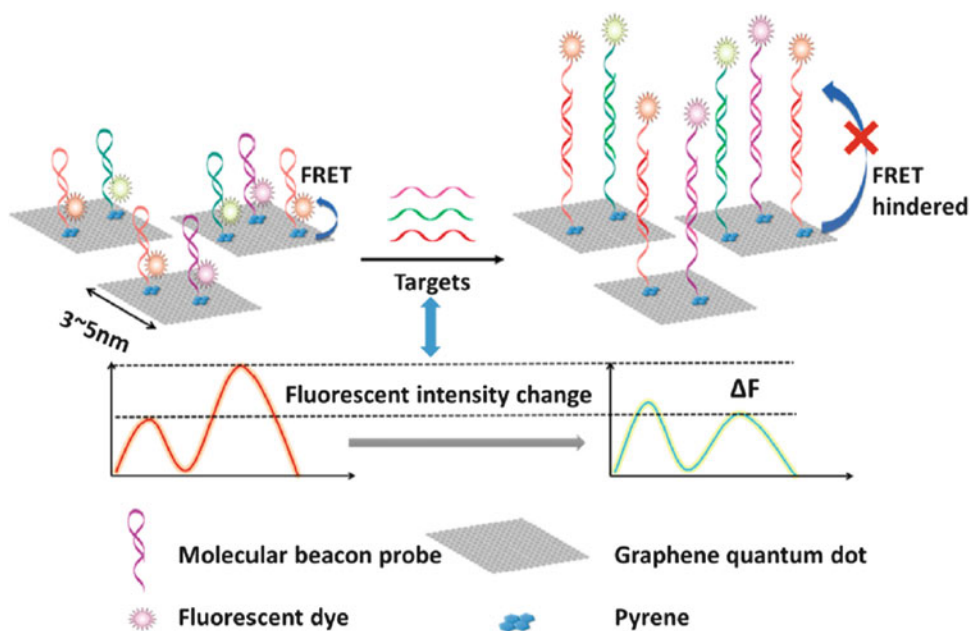


Fig. 4.5 Schematic view illustrating the detection mechanism of the py-MB detection system. (Zhang et al. 2015. Copyright © Zhang H et al.)

analyzed with LOD of 100 pM and dynamic range of 0.1 ~ 200 nM. Pyrene-functionalized MB (py-MB) probes were prepared with 5' modification on pyrene and 3' modification of the fluorescence dyes, Cy3 and Cy5, while leaving the loop part of the sequence complementary to the target miRNA. The π - π interaction between pyrene part of the py-MBs and GQDs tethers the py-MBs on GQDs. When no target miRNAs came in contact with the probe py-MBs, FRET occurs between GQDs and the fluorescence dyes. However, when target miRNAs are added, double strands are formed preventing FRET from occurring.

References

- Alwarappan S, Erdem A, Liu C, Li C-Z (2009) Probing the electrochemical properties of graphene Nanosheets for biosensing applications. *J Phys Chem C* 113 (20):8853–8857. <https://doi.org/10.1021/jp9010313>
- Aparna R, Sivakumar N, Balakrishnan A, Nair AS, Nair SV, Subramanian KRV (2013) An effective route to produce few-layer graphene using combinatorial ball milling and strong aqueous exfoliants. *J Renew Sustain Energy* 5(3):033123–033123. <https://doi.org/10.1063/1.4809794>
- Balandin AA, Ghosh S, Bao W, Calizo I, Teweldebrhan D, Miao F, Lau CN (2008) Superior thermal conductivity of single-layer graphene. *Nano Lett* 8(3):902–907. <https://doi.org/10.1021/nl0731872>
- Bonanni A, Ambrosi A, Pumera M (2012) On oxygen-containing groups in chemically modified Graphenes. *Chem Eur J* 18(15):4541–4548. <https://doi.org/10.1002/chem.201104003>
- Bourlinos AB, Gournis D, Petridis D, Szabó T, Szeri A, Dékány I (2003) Graphite oxide: chemical reduction to graphite and surface modification with primary aliphatic amines and amino acids. *Langmuir* 19 (15):6050–6055. <https://doi.org/10.1021/la026525h>
- Broude NE (2002) Stem-loop oligonucleotides: a robust tool for molecular biology and biotechnology. *Trends Biotechnol* 20(6):249–256. [https://doi.org/10.1016/S0167-7799\(02\)01942-X](https://doi.org/10.1016/S0167-7799(02)01942-X)
- Chan WCW, Nie S (1998) Quantum dot bioconjugates for ultrasensitive nonisotopic detection. *Science* 281 (5385):2016–2018. <https://doi.org/10.1126/science.281.5385.2016>
- Chen W, Yan L, Bangal PR (2010) Preparation of graphene by the rapid and mild thermal reduction of graphene oxide induced by microwaves. *Carbon* 48 (4):1146–1152. <https://doi.org/10.1016/j.carbon.2009.11.037>
- Chen S, Liu J-W, Chen M-L, Chen X-W, Wang J-H (2012) Unusual emission transformation of graphene quantum dots induced by self-assembled aggregation. *Chem Commun* 48(61):7637–7639. <https://doi.org/10.1039/C2CC32984K>

- Choi W, Lahiri I, Seelaboyina R, Kang YS (2010) Synthesis of graphene and its applications: a review. *Crit Rev Solid State Mater Sci* 35(1):52–71. <https://doi.org/10.1080/10408430903505036>
- Ciesielski A, Samori P (2014) Graphene via sonication assisted liquid-phase exfoliation. *Chem Soc Rev* 43(1):381–398. <https://doi.org/10.1039/C3CS60217F>
- Dreyer DR, Park S, Bielawski CW, Ruoff RS (2010) The chemistry of graphene oxide. *Chem Soc Rev* 39(1):228–240. <https://doi.org/10.1039/B917103G>
- Du D, Zou Z, Shin Y, Wang J, Wu H, Engelhard MH, Liu J, Aksay IA, Lin Y (2010) Sensitive Immunosensor for Cancer biomarker based on dual signal amplification strategy of graphene sheets and multienzyme functionalized carbon Nanospheres. *Anal Chem* 82(7):2989–2995. <https://doi.org/10.1021/ac100036p>
- Eda G, Lin Y-Y, Mattevi C, Yamaguchi H, Chen H-A, Chen IS, Chen C-W, Chhowalla M (2010) Blue photoluminescence from chemically derived graphene oxide. *Adv Mater* 22(4):505–509. <https://doi.org/10.1002/adma.200901996>
- Fan L, Hu Y, Wang X, Zhang L, Li F, Han D, Li Z, Zhang Q, Wang Z, Niu L (2012) Fluorescence resonance energy transfer quenching at the surface of graphene quantum dots for ultrasensitive detection of TNT. *Talanta* 101(Suppl C):192–197. <https://doi.org/10.1016/j.talanta.2012.08.048>
- Freeman R, Willner I (2012) Optical molecular sensing with semiconductor quantum dots (QDs). *Chem Soc Rev* 41(10):4067–4085. <https://doi.org/10.1039/C2CS15357B>
- Giovanni M, Bonanni A, Pumera M (2012) Detection of DNA hybridization on chemically modified graphene platforms. *Analyst* 137(3):580–583. <https://doi.org/10.1039/C1AN15910K>
- Hernandez Y, Nicolosi V, Lotya M, Blighe FM, Sun Z, De S, McGovern IT, Holland B, Byrne M, Gun'Ko YK, Boland JJ, Niraj P, Duesberg G, Krishnamurthy S, Goodhue R, Hutchison J, Scardaci V, Ferrari AC, Coleman JN (2008) High-yield production of graphene by liquid-phase exfoliation of graphite. *Nat Nanotechnol* 3:563–568. <https://doi.org/10.1038/nnano.2008.215>
- Hummers WS, Offeman RE (1958) Preparation of graphitic oxide. *J Am Chem Soc* 80(6):1339–1339. <https://doi.org/10.1021/ja01539a017>
- Lai G, Zhang H, Tamanna T, Yu A (2014) Ultrasensitive immunoassay based on electrochemical measurement of enzymatically produced polyaniline. *Anal Chem* 86(3):1789–1793. <https://doi.org/10.1021/ac4037119>
- Lee C, Wei X, Kysar JW, Hone J (2008) Measurement of the elastic properties and intrinsic strength of monolayer graphene. *Science* 321(5887):385–388. <https://doi.org/10.1126/science.1157996>
- Li D, Müller MB, Gilje S, Kaner RB, Wallace GG (2008) Processable aqueous dispersions of graphene nanosheets. *Nat Nanotechnol* 3:101–105. <https://doi.org/10.1038/nnano.2007.451>
- Li X, Cai W, An J, Kim S, Nah J, Yang D, Piner R, Velamakanni A, Jung I, Tutuc E, Banerjee SK, Colombo L, Ruoff RS (2009) Large-area synthesis of high-quality and uniform graphene films on copper foils. *Science* 324(5932):1312–1314. <https://doi.org/10.1126/science.1171245>
- Li Y, Hu Y, Zhao Y, Shi G, Deng L, Hou Y, Qu L (2011) An electrochemical avenue to green-luminescent graphene quantum dots as potential Electron-acceptors for photovoltaics. *Adv Mater* 23(6):776–780. <https://doi.org/10.1002/adma.201003819>
- Li L-L, Ji J, Fei R, Wang C-Z, Lu Q, Zhang J-R, Jiang L-P, Zhu J-J (2012) A facile microwave avenue to Electrochemiluminescent two-color graphene quantum dots. *Adv Funct Mater* 22(14):2971–2979. <https://doi.org/10.1002/adfm.201200166>
- Liu F, Ming P, Li J (2007) Ab initio. *Phys Rev B* 76(6):064120–064120
- Liu R, Wu D, Feng X, Müllen K (2011) Bottom-up fabrication of Photoluminescent graphene quantum dots with uniform morphology. *J Am Chem Soc* 133(39):15221–15223. <https://doi.org/10.1021/ja204953k>
- Lu J, J-x Y, Wang J, Lim A, Wang S, Loh KP (2009) One-pot synthesis of fluorescent carbon nanoribbons, nanoparticles, and graphene by the exfoliation of graphite in ionic liquids. *ACS Nano* 3(8):2367–2375. <https://doi.org/10.1021/nn900546b>
- Mayorov AS, Gorbachev RV, Morozov SV, Britnell L, Jalil R, Ponomarenko LA, Blake P, Novoselov KS, Watanabe K, Taniguchi T, Geim AK (2011) Micrometer-scale ballistic transport in encapsulated graphene at room temperature. *Nano Lett* 11(6):2396–2399. <https://doi.org/10.1021/nl200758b>
- Michalet X, Pinaud FF, Bentolila LA, Tsay JM, Doose S, Li JJ, Sundaresan G, Wu AM, Gambhir SS, Weiss S (2005) Quantum dots for live cells, in vivo imaging, and diagnostics. *Science* 307(5709):538–544. <https://doi.org/10.1126/science.1104274>
- Monsur A, Haque J, Park H, Sung D, Jon S, Choi S-Y, Kim K (2012) An electrochemically reduced graphene oxide-based electrochemical Immunosensing platform for ultrasensitive antigen detection. *Anal Chem* 84:1871–1878. <https://doi.org/10.1021/ac202562v>
- Nair RR, Blake P, Grigorenko AN, Novoselov KS, Booth TJ, Stauber T, Peres NMR, Geim AK (2008) Fine structure constant defines visual transparency of graphene. *Science* 320(5881):1308–1308. <https://doi.org/10.1126/science.1156965>
- Niyogi S, Bekyarova E, Itkis ME, McWilliams JL, Hamon MA, Haddon RC (2006) Solution properties of graphite and graphene. *J Am Chem Soc* 128(24):7720–7721. <https://doi.org/10.1021/ja060680r>
- Niyogi S, Bekyarova E, Itkis ME, Zhang H, Shepperd K, Hicks J, Sprinkle M, Berger C, Lau CN, deHeer WA, Conrad EH, Haddon RC (2010) Spectroscopy of covalently functionalized graphene. *Nano Lett* 10(10):4061–4066. <https://doi.org/10.1021/nl1021128>
- Novoselov KS, Geim AK, Morozov SV, Jiang D, Zhang Y, Dubonos SV, Grigorieva IV, Firsov AA

- (2004) Electric field effect in atomically thin carbon films. *Science* 306(5696):666–669. <https://doi.org/10.1126/science.1102896>
- Pan D, Zhang J, Li Z, Wu M (2010) Hydrothermal route for cutting graphene sheets into blue-luminescent graphene quantum dots. *Adv Mater* 22(6):734–738. <https://doi.org/10.1002/adma.200902825>
- Paredes JI, Villar-Rodil S, Martínez-Alonso A, Tascón JMD (2008) Graphene oxide dispersions in organic solvents. *Langmuir* 24(19):10560–10564. <https://doi.org/10.1021/la801744a>
- Qian ZS, Shan XY, Chai LJ, Ma JJ, Chen JR, Feng H (2014) A universal fluorescence sensing strategy based on biocompatible graphene quantum dots and graphene oxide for the detection of DNA. *Nanoscale* 6(11):5671–5674. <https://doi.org/10.1039/C3NR06583A>
- Sinitskii A, Dimiev A, Corley DA, Fursina AA, Kosynkin DV, Tour JM (2010) Kinetics of Diazonium functionalization of chemically converted graphene nanoribbons. *ACS Nano* 4(4):1949–1954. <https://doi.org/10.1021/nn901899j>
- Skaltsas T, Ke X, Bittencourt C, Tagmatarchis N (2013) Ultrasonication induces oxygenated species and defects onto exfoliated graphene. *J Phys Chem C* 117(44):23272–23278. <https://doi.org/10.1021/jp4057048>
- Smith AM, Nie S (2010) Semiconductor nanocrystals: structure, properties, and band gap engineering. *Acc Chem Res* 43(2):190–200. <https://doi.org/10.1021/ar9001069>
- Stankovich S, Dikin DA, Dommett GHB, Kohlhaas KM, Zimney EJ, Stach EA, Piner RD, Nguyen ST, Ruoff RS (2006) Graphene-based composite materials. *Nature* 442:282–286. <https://doi.org/10.1038/nature04969>
- Stobiecka M, Chałupa A (2015) Biosensors based on molecular beacons. *Chem Pap* 69(1):62–76. <https://doi.org/10.1515/chempap-2015-0026>
- Tang L, Wang Y, Li Y, Feng H, Lu J, Li J (2009) Preparation, structure, and electrochemical properties of reduced graphene sheet films. *Adv Funct Mater* 19(17):2782–2789. <https://doi.org/10.1002/adfm.200900377>
- Wang J, Chen J, Chang P, LeBlanc A, Li D, Abbruzzese JL, Frazier ML, Killary AM, Sen S (2009a) MicroRNAs in plasma of pancreatic ductal adenocarcinoma patients as novel blood-based biomarkers of disease. *Cancer Prev Res* 2(9):807–813. <https://doi.org/10.1158/1940-6207.capr-09-0094>
- Wang H, Robinson JT, Li X, Dai H (2009b) Solvothermal reduction of chemically exfoliated graphene sheets. *J Am Chem Soc* 131(29):9910–9911. <https://doi.org/10.1021/ja904251p>
- Wang K, Tang Z, Yang CJ, Kim Y, Fang X, Li W, Wu Y, Medley CD, Cao Z, Li J, Colon P, Lin H, Tan W (2009c) Molecular engineering of DNA: molecular beacons. *Angew Chem Int Ed* 48(5):856–870. <https://doi.org/10.1002/anie.200800370>
- Wang Z, Zhang J, Chen P, Zhou X, Yang Y, Wu S, Niu L, Han Y, Wang L, Chen P, Boey F, Zhang Q, Liedberg B, Zhang H (2011) Label-free, electrochemical detection of methicillin-resistant staphylococcus aureus DNA with reduced graphene oxide-modified electrodes. *Biosens Bioelectron* 26(9):3881–3886. <https://doi.org/10.1016/j.bios.2011.03.002>
- Yan X, Cui X, Li L-s (2010) Synthesis of large, stable colloidal graphene quantum dots with tunable size. *J Am Chem Soc* 132(17):5944–5945. <https://doi.org/10.1021/ja1009376>
- Yang T, Li Q, Li X, Wang X, Du M, Jiao K (2013) Freely switchable impedimetric detection of target gene sequence based on synergistic effect of ERGNO/PANInanocomposites. *Biosens Bioelectron* 42(Suppl C):415–418. <https://doi.org/10.1016/j.bios.2012.11.007>
- Zhang M, Bai L, Shang W, Xie W, Ma H, Fu Y, Fang D, Sun H, Fan L, Han M, Liu C, Yang S (2012) Facile synthesis of water-soluble, highly fluorescent graphene quantum dots as a robust biological label for stem cells. *J Mater Chem* 22(15):7461–7467. <https://doi.org/10.1039/C2JM16835A>
- Zhang H, Wang Y, Zhao D, Zeng D, Xia J, Aldabahi A, Wang C, San L, Fan C, Zuo X, Mi X (2015) Universal fluorescence biosensor platform based on graphene quantum dots and pyrene-functionalized molecular beacons for detection of MicroRNAs. *ACS Appl Mater Interfaces* 7(30):16152–16156. <https://doi.org/10.1021/acsami.5b04773>
- Zhao H, Chang Y, Liu M, Gao S, Yu H, Quan X (2013) A universal immunosensing strategy based on regulation of the interaction between graphene and graphene quantum dots. *Chem Commun* 49(3):234–236. <https://doi.org/10.1039/C2CC35503E>
- Zhou M, Zhai Y, Dong S (2009) Electrochemical sensing and biosensing platform based on chemically reduced graphene oxide. *Anal Chem* 81(14):5603–5613. <https://doi.org/10.1021/ac900136z>
- Zhu Y, Murali S, Stoller MD, Velamakanni A, Piner RD, Ruoff RS (2010) Microwave assisted exfoliation and reduction of graphite oxide for ultracapacitors. *Carbon* 48(7):2118–2122. <https://doi.org/10.1016/j.carbon.2010.02.001>
- Zhu S, Zhang J, Qiao C, Tang S, Li Y, Yuan W, Li B, Tian L, Liu F, Hu R, Gao H, Wei H, Zhang H, Sun H, Yang B (2011) Strongly green-photoluminescent graphene quantum dots for bioimaging applications. *Chem Commun* 47(24):6858–6860. <https://doi.org/10.1039/C1CC11122A>
- Zhu S, Zhang J, Liu X, Li B, Wang X, Tang S, Meng Q, Li Y, Shi C, Hu R, Yang B (2012) Graphene quantum dots with controllable surface oxidation, tunable fluorescence and up-conversion emission. *RSC Adv* 2(7):2717–2720. <https://doi.org/10.1039/C2RA20182H>